FEASIBILITY OF SELF-REINFORCED CONCRETE BLOCK FOR IMPROVED DUCTILITY

M. P. Joyal[1], M. J. Tait[2] and R. G. Drysdale[3]

[1] M.A.Sc. Candidate, Department of Civil Engineering, McMaster University, Hamilton, ON, L8S 4L7, Canada, joyalmp@mcmaster.ca

[2] Joe Ng/JNE Consulting Chair in Design, Construction and Management in Infrastructure Renewal, Center for Effective Design of Structures, Department of Civil Engineering, Hamilton, ON, L8S 4L7, Canada, taitm@mcmaster.ca

[3] Professor Emeritus, Centre for Effective Design of Structures, Department of Civil Engineering, Hamilton, ON, L8S 4L7, Canada, drysdale@mcmaster.ca

ABSTRACT

A study was undertaken to assess the feasibility and effectiveness of lateral confining devices molded into concrete block for improved ductility. Production trials of the proposed Self-Reinforced Concrete Block (SR Block) have demonstrated that the reinforcing devices can be molded into the concrete during manufacture of the block with full compaction of the concrete achieved. This internal reinforcement provides lateral confinement to the enclosed volume of block and grout. The resulting triaxial state of compressive stress under axial load allows increased axial compressive strains to be developed along with increased compressive strength of the confined volume. A preliminary series of prism tests were conducted to compare the performance of SR Block to similar unreinforced block prism specimens. The results indicate improved plasticity due to the presence of the confining devices within the block. Despite spalling of the unconfined portions of the block at high strains, the SR Block specimens retained load carrying capacities in excess of the peak capacity of similar unreinforced/unconfined block prisms at strains beyond 2% with no visible damage to the confining devices.

KEYWORDS: compressive strain, concrete block, confinement, ductility, self-reinforced, seismic performance

INTRODUCTION

In Canada and worldwide, the economic competitiveness of concrete masonry for conditions where design is controlled by seismic loading has been limited. This is related to the low crushing strain characteristics of concrete block, which may limit the achievable level of ductility. However, as reviewed below, some previous research has demonstrated the beneficial effect of various types of confinement on the ductility and compressive strength capacity of concrete block. The goal of this research is to present a new application of confinement in the form of Self-Reinforced Concrete Block (SR Block).

In this regard, past work related to increasing the ductility of concrete masonry has focused on lateral confinement techniques which are external to the block. The Priestly Plate [1] and various wire mesh techniques [2,3] involve devices placed within the bed mortar joint between courses and, while they have been successful in providing confinement, rely on consistency of placement by a mason on-site. Other techniques involve placing confinement within the block cell including

spiral reinforcement [2,4] and polymer fibres [5]. The placing of steel devices within the cell resulted in hindered performance due to incomplete grout consolidation around the device [4]. Tests with polymer fibres as confinement reported improvements in strain capacity similar to other, previously tested forms of confinement [5]. Beyond masonry research there is a precedent of concrete columns laterally confined with continuous spiral reinforcement [6] to provide lateral support for the vertical bars and to confine the enclosed concrete resulting in enhanced compressive strength and failure strain.

This study follows some preliminary research [7] which provided proof of concept. It documents success of a previously untried method of molding steel confining devices into concrete block during the standard block manufacturing process. This paper assesses the feasibility of this process for mass production; the results of axial compression tests on prisms constructed from SR Block are compared to similar unreinforced specimens.

DEVICE DESIGN

Drawing from previous research related to confinement in concrete columns [6,8], the most effective shape for confinement was determined to be a circular device running the height of the block to form a semi-continuous column of confined material over several courses of block. The mortar, block, and grout in the local region of the mortar bed joints depend on the near proximity of devices above and below for confinement. A 6 mm clearance from the bottom of the block to the confining device allows a 6 mm notch to be formed in the block webs which, when combined with the 10 mm mortar bed joint, permits positioning of up to 10 mm diameter horizontal reinforcement in walls.

For this study, the selected confining devices were fabricated from 2.90 mm thick sheet steel with 19.1 mm square punched holes. The width of the strips on all sides of the punched holes was 6.3 mm. The sheets were cut to a height of 184 mm, allowing 6 mm of clearance at the bottom of the finished block. The 514 mm long sheet was wrapped into a tubular shape with an outside diameter of 167 mm and the tube was welded along the abutting vertical end strips to complete the confining device shown in Figure 1.

The horizontal strips of the cage provide the desired confining hoops while the vertical strips provide stiffness of the cage during compaction of concrete in the mold. The openings in the cage between strips were maximized to enhance concrete filling of the block mold and to facilitate bond between the outer concrete and the enclosed concrete. The size of the strips was chosen to ensure that the high strain compressive capacity of the confined volume would equal or exceed capacity of similar unreinforced/unconfined block masonry.

Figure 1: Confining Device

BLOCK MAKING

In order to increase the effectiveness of the confining device by maximizing the volume of enclosed concrete, it was necessary to fit the largest possible cylindrical confining device around each block cell while leaving sufficient clearance inside and outside of the device to facilitate placement and compaction of the zero slump concrete. In these first trials conducted before it was confirmed that such placement and compaction did not present a significant problem, a prototype block with small circular cells was designed. Using a standard 20 cm splitter block mold (190 mm x 190 mm x 390 mm), new mold inserts were machined to create 101.6 mm diameter cells to replace the more traditional tapered, pear-shaped cells. This mold maximized the volume of enclosed block concrete while still allowing sufficient space in the cells to install vertical reinforcement and grout. The cells were positioned to ensure vertical alignment in a typical running bond pattern so that the confined volume would provide a straight member after spalling of the outer shell.

Manufacture of the SR Block and similar block without confining devices was performed in an automated plant used for commercial mass production of masonry units. The production line, using a "Besser" block machine, compacts a zero-slump concrete into three block molds during each cycle. For this study, prototype blocks with and without the confining device were produced from the same batch of concrete to ensure consistent properties for test comparisons. To manufacture the SR Blocks, the production line was paused to allow manual centring of the confining devices on the base plate beneath the prototype mold. After positioning, the manufacturing process resumed and the base plate was raised into position under the mold where it was filled with concrete and vibrated for compaction.

To check that the concrete was being properly compacted and voids around the confining device were filled, in the first production runs, the device was exposed by removing a portion of the face-shell concrete to permit visual inspection of some trial blocks. As shown in Figure 2, compaction of the concrete was complete; the confining device was not deformed during the manufacturing process. This block production trial indicated that with some streamlining, mass production of SR Block is feasible with existing manufacturing processes.

Figure 2: SR Block During Manufacturing with Confining Device Exposed by Removal of Compacted Exterior Concrete

EXPERIMENTAL PROGRAM

For this paper, two series of masonry prisms tested under axial compressive loads are examined to assess the effect of using confining devices within concrete block. In order to avoid the effects of end confinement due to hard capping and to simulate failure patterns expected in walls, four-course high prisms with a running bond were constructed by an experienced mason. The three prisms in each series were constructed using the 101.6 mm cell, 20 cm prototype blocks described above and all were grouted with fine grout mixed in the laboratory. The geometry of the flat end, two-cell splitter blocks was the same for both series but the first series did not have confining devices molded into the blocks. The properties of each constituent material are listed in Table 1.

Table 1: Material Properties

Material	Average Strength (MPa)	C.O.V. (%)	Yield Strength (MPa)
Block	29.2	-	-
Mortar	14.6	8.9	-
Grout (Cylinder)	24.3	10.2	-
Grout (Cell-Moulded)	32.2	8.2	-
Steel (device)	559.5	-	400.9

Mortar Mix (weight ratio) cement: lime: dry masonry sand: water = 1.00: 0.21: 4.39: 0.95
Grout Mix (weight ratio) cement: lime: dry sand: water = 1.00: 0.04: 4.00: 0.85

Following an average 67-day curing period in the dry laboratory environment, the prisms were capped at the top and bottom with a thin layer of high strength gypsum cement (hydrostone) and bonded to 76.2 mm steel plates. This capping procedure fulfils the ASTM C140 requirements [9] for capping of standard masonry prisms.

Capped prisms were loaded using a servo-hydraulically controlled testing machine (Figure 3) with capacity of 2500 kN. Within the setup, each prism was vertically levelled and centred beneath a spherically seated loading head to ensure concentric loading.

Once centred within the test setup, each prism was instrumented with a series of eight 50 mm range, draw-wire potentiometers to measure average strains over the height of the specimen. The first four potentiometers (one located on each side of the specimen) spanned a 600 mm gauge length from the mid-height of the top block to mid-height of the bottom block of the prism and were mounted directly onto the block. These potentiometers gave representative strain readings up to the initiation of cracking and spalling of the outer shell of the blocks, without being influenced by the confining effects of the steel platen at the top and bottom of the specimen. The second set of four potentiometers spanned from the bottom plate of the test setup to the top plate on each side of the specimen to read strain over the full height of the prism. Although influenced by confining effects from the hard capping of the prism, these potentiometers continued to provide relevant readings in the post-cracking stages of the test. Readings from this latter group of potentiometers were found to agree very closely with results from those located directly on the block.

Figure 3: Prism in Testing Machine

A second form of instrumentation provided validation of the readings obtained from the draw-wire potentiometers at low strains. One specimen in each series was also outfitted with gauge points for a demountable mechanical (Demec) strain gauge over a mid-height 200 mm gauge length. Manual measurements at regular intervals up to 50% of maximum load yielded results which closely agreed with the digital output from the draw-wire potentiometers, verifying that the results from the draw-wire potentiometers were sufficient for the remainder of the tests.

Following instrumentation, the specimens were subjected to vertical compression under displacement (strain) control in order to obtain a complete stress-strain curve for each test. The loading (bottom) head of the machine was set to travel at a constant rate of approximately 0.9 mm/min corresponding to an average strain rate of 0.0011 per minute. Output from three load cells, visible above the top head of the machine in Figure 3, were combined to obtain load readings throughout the test. Load cell and potentiometer outputs were recorded at a sampling frequency of 2 Hz. To obtain stress-strain curves for each specimen, load readings were divided by the total grouted area of the block prism (74100 mm^2) and potentiometer readings were divided by their respective gauge lengths as measured prior to each test. An average of the strain readings gained from the potentiometers on each of the four sides of the prism provided average strain reading across the specimen.

TEST RESULTS AND ANALYSIS

The first test series consisted of three fully grouted, unreinforced, prototype block prisms. The failure stress and strain characteristics for the specimens are shown in Table 2.

Table 2: Unreinforced Prism Series Results

Test Number	Peak Stress			Strain at Peak Stress		
	Individual (MPa)	Average (MPa)	C.O.V. (%)	Individual	Average	C.O.V. (%)
1	17.7	16.7	6.3	0.0021	0.0021	12.2
2	15.6			0.0023		
3	16.7			0.0018		

Failure patterns for these specimens were consistent, initiating with vertical cracking along each face, observed between 40% and 50% of the ultimate load. The vertical cracks led to splitting of the face shell concrete, spalling away from the grout columns, which then crushed under the load. Failure of the prisms was rapid following peak load, demonstrating the brittle behaviour characteristic of unreinforced masonry. Figure 4 shows the typical failure patterns of the unreinforced prisms.

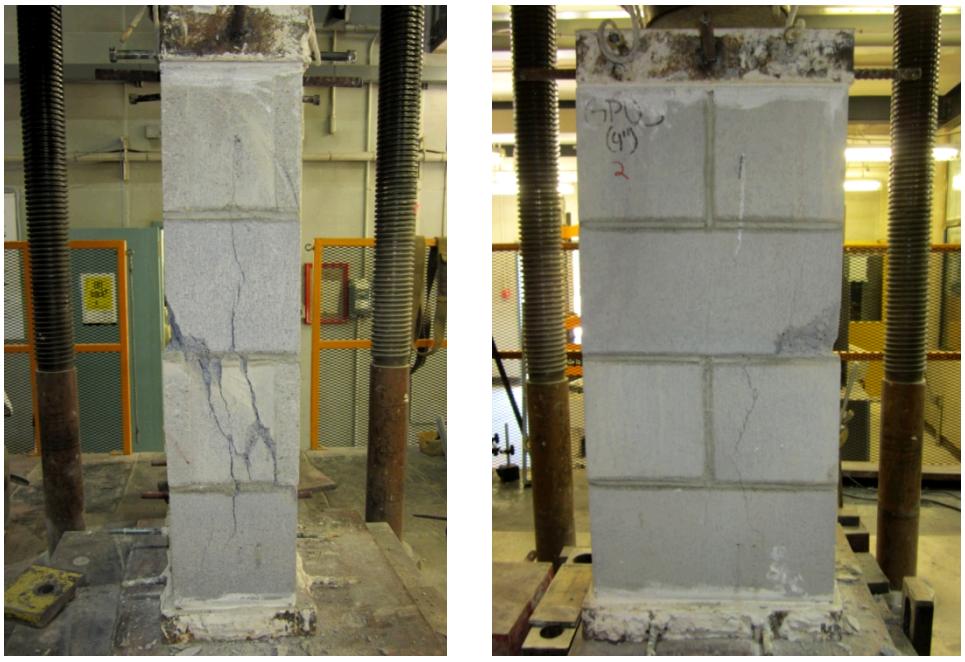

a) End View **b) Face View**

Figure 4: Typical Failure Patterns of Unreinforced Specimens.

The second test series consisted of three fully grouted, self-reinforced, prototype block prisms. An error during testing of the first prism in this series resulted in a very rapid loading rate up to the initial point of face shell spalling. Although the issue was resolved and the prescribed loading rate was resumed for the remainder of the test, the initial rapid loading resulted in a higher-than-expected initial peak loading value. While all three tests followed the same stress-strain curve

shape and had similar values for Young's modulus, the values obtained from the second and third tests were more in line with one another. It is for this reason that a second average value, excluding values from the first test, is presented along with the overall statistics in Table 5. It is also for this reason that a representative stress-strain plot rather than an average plot is used to display test data.

Failure patterns for the specimens in this test series were also consistent. As observed with the unreinforced specimens, vertical cracking initiated at approximately 50% of the failure load and extended to cause splitting of the face shell concrete outside of the confining device, allowing this concrete to spall off. Figure 5 displays the cracking/spalling pattern typically observed at this stage of the self-reinforced specimen tests.

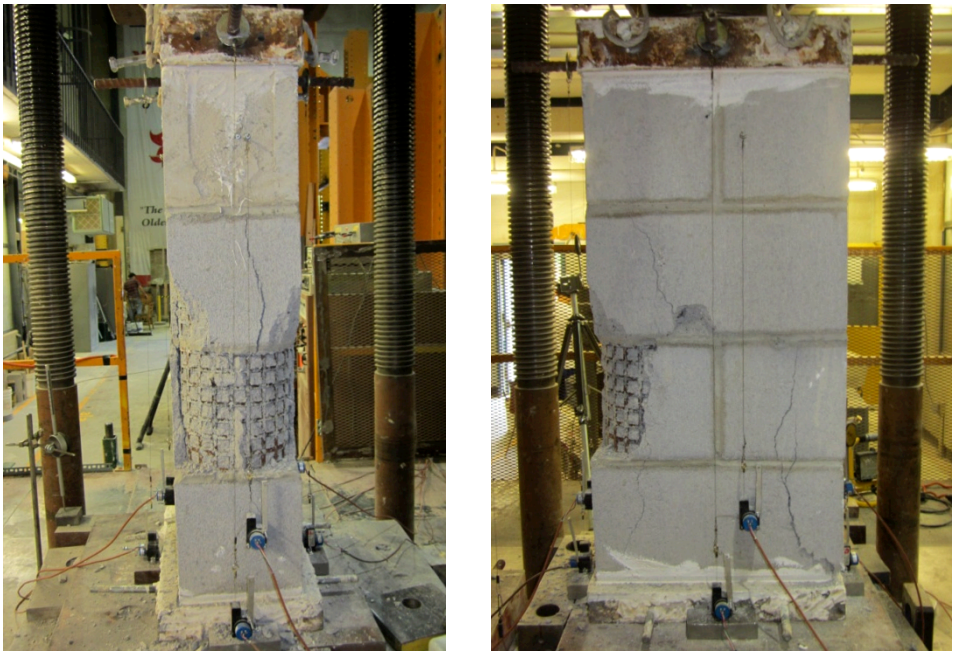

a) End View **b) Face View**

Figure 5: Typical Initial Splitting/Spalling Patterns of Self-Reinforced Specimens.

The first load peak for the self-reinforced specimens occurred as the concrete split, at a similar strain to what was observed with the unreinforced specimens. After this peak, each prism experienced a slight drop in capacity (5% to 10%) as the concrete on the outside of the confining device began to spall. As the specimen continued to undergo increasing strain, the prisms regained strength up to and surpassing the original peak capacity. This second peak, occurring at an average of about 1% strain, indicated the capacity of the confined concrete and grout enclosed within the confining devices. This peak was followed by a gradual decrease in capacity as the specimen continued to undergo increasing strain, resulting in a very ductile failure of the prism. At the very large average strain of 2%, the prisms still retained a capacity equal to the peak capacity of the unreinforced prisms. Even at strains of over 3%, the confined volume of grout and concrete block remained intact with significant reserve compressive capacity. Data for the peak responses are presented in Table 3.

Table 3: Self-Reinforced Prism Series Results

Test Number	Individual (MPa)	Average (MPa)	C.O.V. (%)	Average Excluding Test 1 (MPa)	Individual	Average	C.O.V. (%)	Average Excluding Test 1
	Initial Peak Stress				Strain at Initial Peak Stress			
1 2 3	20.6 17.5 18.2	18.8	8.7	17.9	0.0024 0.0034 0.0021	0.0026	25.8	0.0028
	Second Peak Stress				Strain at Second Peak Stress			
1 2 3	20.5 18.5 18.9	19.3	5.5	18.7	0.010 0.008 0.013	0.010	24.4	0.011
	Stress at 2% Strain				Stress (MPa) at 3% Strain			
1 2 3	16.6 16.8 16.6	16.7	0.7	16.7	14.6 13.5 13.5	13.9	4.6	13.5

Although drift limitations in shear wall buildings make it unlikely that strains up to 2% can be utilized in seismic design, to observe ultimate failure patterns, loading of the SR block specimens was continued until the prism capacity dropped to 50% of the peak load. The drop in capacity to this point occurred due to yielding of the steel confining devices.

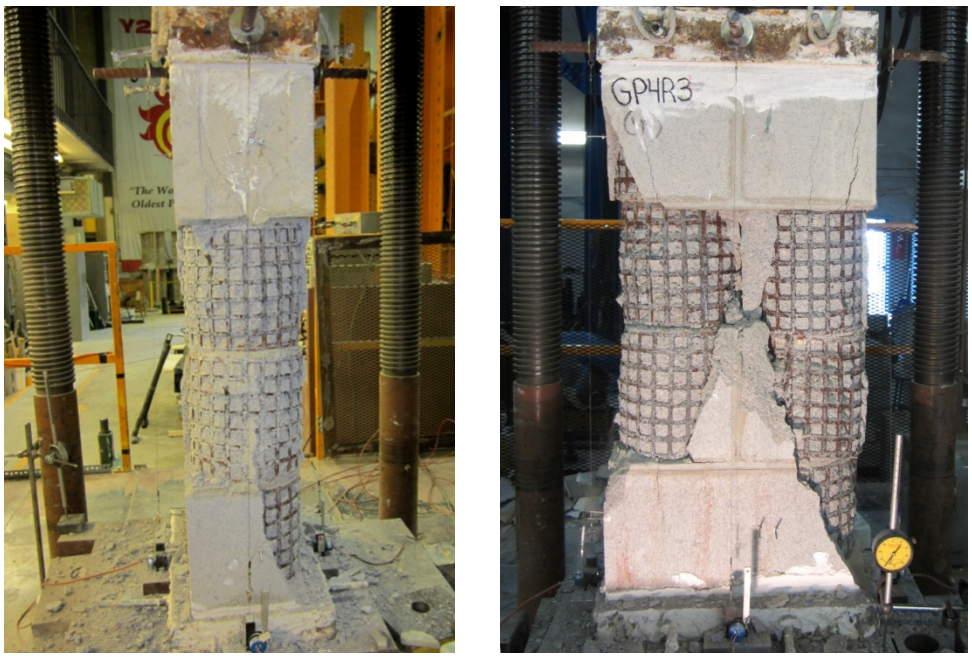

a) End View **b) Face View**

Figure 6: Self-Reinforced Specimen at 2% Strain.

Representative stress-strain curves for the unreinforced and SR Block prism series were plotted in Figure 7. These curves indicate that, within the elastic loading range of the prisms (prior to cracking of the face shell concrete), the presence of the confining device has little influence on the characteristics of the prism. At the initial peak stress, the approximately 10% increase in SR Block prism strength can be attributed to the presence of the steel confining devices acting as vertical reinforcement but otherwise both specimens follow the same pattern up to the initial peak capacity. Following the initial peak, both curves show a decline in capacity, but while the unreinforced specimen rapidly lost all capacity at a strain of approximately 0.3%, the self-reinforced specimen regained strength. As the enclosed concrete and grout underwent vertical strain, the resulting lateral expansion against the confining device created a triaxial compression state of stress in the confined concrete and grout which enhanced the vertical compressive strength of this remaining 57% of the original cross-section. This beneficial effect was sufficient to allow full capacity to be regained and maintained up to very high strain levels.

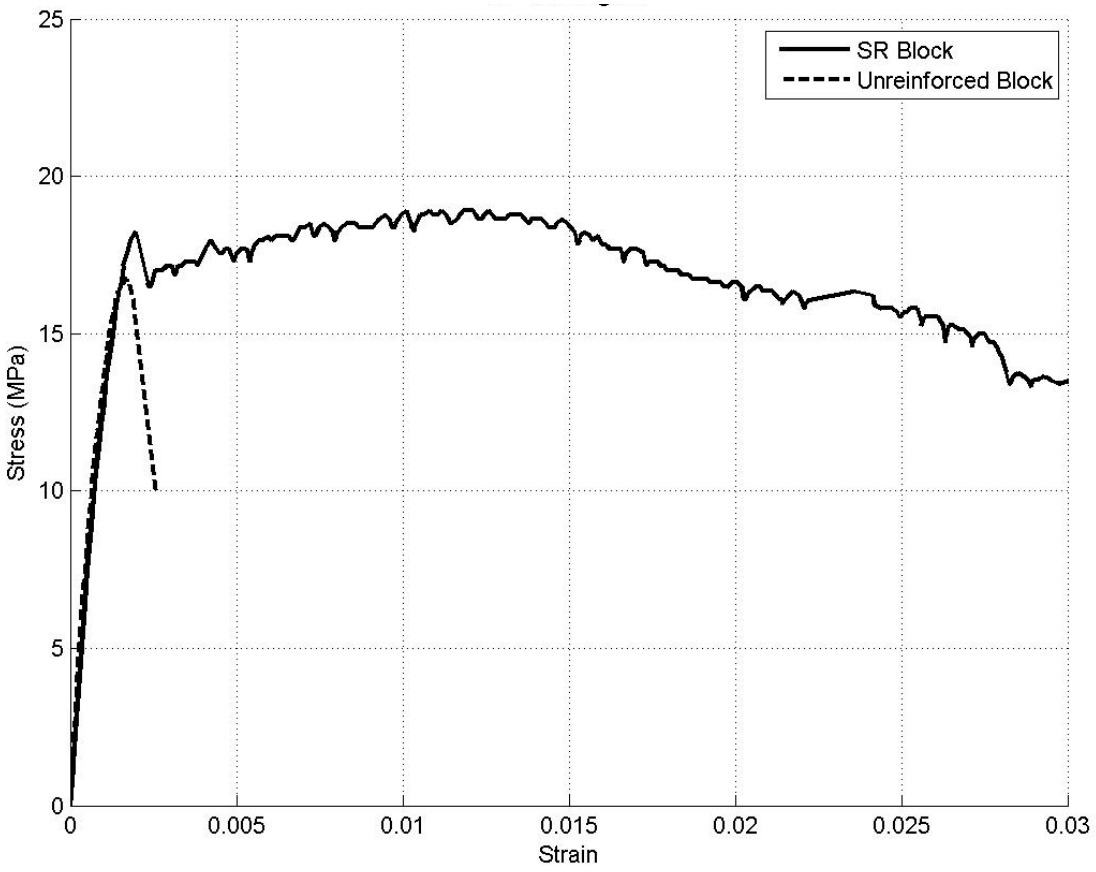

Figure 7: Comparison of Representative Stress-Strain Curves for Self- Reinforced and Unreinforced Prisms

CONCLUSIONS

Block plant trials demonstrated that it is possible to mold confining devices within concrete block without requiring adjustments to the mix design or the manufacturing equipment. Inspection of the blocks confirmed that full compaction of the concrete was achieved and the

block strength was not impaired by the presence of the confining devices. From these trials, it was determined that mass production of SR Block is feasible with existing facilities.

In these tests, as a precaution to help ensure the best chance of achieving full compaction of the concrete around the confining device, small 101.6 mm diameter cells were used to leave relatively large minimum web and face shell thicknesses. It was thought that the resulting reduced resistance to compaction would enhance compaction around the confining devices. However, the resulting 77% solid units, each weighing approximately 23 kg, were well above the weight normally placed by a lone mason. Subsequent block plant tests have shown that the cell size can be increased to match traditional hollow block without adversely affecting block compaction.

Comparison of test results of the SR Block to similar unreinforced prisms show that despite spalling of the face shell concrete outside of the confining device, the SR Block specimens retained load carrying capacity in excess of the peak capacity of their unreinforced counterparts and were able to retain at least the capacity of the unreinforced counterparts up to 2% strain. In this regard, although retention of the full initial peak capacity following development of very high compressive strains provides very strong evidence of the potential for this technique to dramatically increase ductility and energy dissipation of reinforced masonry, there are possible cost-saving refinements. If retention of 80% of peak compressive capacity at high strains (and correspondingly higher percentages of related shear wall capacities) is deemed satisfactory, a reduction in the amount of confinement required would reduce the cost of confining devices.

This phase of the test program has confirmed the feasibility and effectiveness of SR block in increasing the ductility and capacity of masonry construction. The next phases of this test program will aim to streamline the manufacturing process and optimize the block and confining device design for applications requiring increased ductility in seismic design.

ACKNOWLEDGEMENTS

The research presented in this paper was funded by the Natural Science and Engineering Research Council of Canada. Provision of mason time by the Ontario Masonry Contactors Association (OMCA) and the Canada Masonry Design Centre is appreciated. Block manufacture and time contributed by Paul Hargest and Boehmers Block is also appreciated.

REFERENCES

1. Priestley, M.J.N. (1981). “Ductility of Unconfined and Confined Concrete Masonry Shear Walls”, The Masonry Society Journal, July-December, p. 28-39.
2. Hart, G.C., Noland, J., Kingsley, G.R. and Englekirk, R. (1988). “The Use of Confinement Steel to Increase the Ductility in Reinforced Concrete Masonry Shear Walls”, The Masonry Society Journal, July-December, p. 19-42.
3. Malmquist, K.J., “Influence of Confinement Reinforcement on the Confinement Reinforcement on the Compressive Behavior of Concrete Block Masonry and Clay Brick Masonry Prisms”, M.S. Thesis, Washington State University, June 2004.

4. Paturova, A., Sparling, B.F. and Wegner, L.D. (2009). “Influence of Vertical Reinforcement and Lateral Confinement on the Axial Capacity of Masonry Walls”, 11th Canadian Masonry Symposium, Toronto, Ontario, Canada.
5. Hervillard, T., McLean, D., Pollock, D. and McDaniel, C. (2005). “Effectiveness of Polymer Fibres for Improving Ductility in Masonry”, 10th Canadian Masonry Symposium, Banff, Alberta, Canada.
6. MacGregor, J.G. and Bartlett, F.M. (1997). “Reinforced Concrete: Mechanics and Design”, Prentice Hall.
7. Toopchi-Nezhad, H., Drysdale, R.G. and Tait, M.J. (2010). “Compression Behaviour of Grouted Concrete Block Prisms Constructed Using Laterally Confined (Self-Reinforced) Concrete Block”, Research Report, Department of Civil Engineering, McMaster University, Hamilton, Ontario, Canada.
8. Mander, J.B., Priestley, M.J.N. and Park, R. (1988). “Observed Stress-Strain Behaviour of Confined Concrete”, Journal of Structural Engineering, Vol. 114, No. 8.
9. ASTM C140-12a, “Standard Test Methods for Sampling and Testing Concrete Masonry Units and Related Units”, ASTM, Conshohocken, PA.